Magnetic and structural transitions in La1−xSrxMnO3: T-x phase diagram

A. A. Mukhin, V. Yu. Ivanov, V. D. Travkin, S. P. Lebedev, Andrei Pimenov, Alois Loidl, A. M. Balbashov

Angaben zur Veröffentlichung / Publication details:

Mukhin, A. A., V. Yu. Ivanov, V. D. Travkin, S. P. Lebedev, Andrei Pimenov, Alois Loidl, and A. M. Balbashov. 1998. "Magnetic and structural transitions in La1−xSrxMnO3: T-x phase diagram." *Journal of Experimental and Theoretical Physics Letters* 68 (4): 356–62. https://doi.org/10.1134/1.567873.

Magnetic and structural transitions in $La_{1-x}Sr_xMnO_3$: $T \pm x$ phase diagram

A. A. Mukhin,[a] V. Yu. Ivanov, V. D. Travkin, and S. P. Lebedev
Institute of General Physics, Russian Academy of Sciences, 117942 Moscow, Russia

A. Pimenov and A. Loidl
Universität Augsburg, D-86159 Augsburg, Germany

A. M. Balbashov
Moscow Power Engineering Institute, 105835 Moscow, Russia

Currently there is a great deal of interest in the investigation of substituted manganites $R_{1-x}A_xMnO_3$, where R is a rare earth and A =Ca,Sr, . . . This is due to the discovery of colossal magnetoresistance[1] as well as diverse magnetic and structural phase transformations[2,3] in these materials. These compounds all have the property that on doping with divalent Ca and Sr ions their magnetic structure changes from antiferromagnetic (with weak ferromagnetism) at $x=0$ to ferromagnetic at $x=0.2\pm0.3$, and their resistance decreases strongly.[2] Their crystal structure also undergoes a number of transformations. For example, as the Sr content in $La_{1-x}Sr_xMnO_3$ increases, the crystal symmetry changes from orthorhombic to rhombohedral, and in the intermediate Sr concentration range $x=(0.1\pm0.15)$ an unusual polaron-ordered state is observed, which neutron diffraction data[4] show to be due to an ordered arrangement of heterovalent ions Mn^{3+}/Mn^{4+} in alternating (001) planes and to the formation of a corresponding superstructure.

$T \pm x$ diagrams which, to a certain extent, take into account the observed phase

transformations in $La_{1-x}Sr_xMnO_3$ have been proposed in a number of works.[4±7] However, these investigations were performed for a small set of compositions and in a limited temperature interval, so that the phase diagrams are mainly of a schematic character, and in some places they even contradict one another (see, for example, Refs. 4, 5, and 7).

In the present work complete investigations were performed of the magnetic and structural phase transitions in $La_{1-x}Sr_xMnO_3$ in a wide interval of temperatures (up to 1050 K) and concentrations ($0 \leqslant x \leqslant 0.45$) on the basis of measurements of their static (magnetization, susceptibility, resistance, magnetoresistance) and submillimeter dynamic properties (permittivity, conductivity). Speci®cally, the permittivity was observed to increase strongly at phase transitions to a polaron-ordering state, and for lightly doped compositions two structural phase transformations were observed at high temperatures. As a result, the complete $T \pm x$ phase diagram of the system was constructed.

We investigated $La_{1-x}Sr_xMnO_3$ ($0 \leqslant x \leqslant 0.45$) single crystals grown by the ¯oating-zone method with radiation heating. The resistivity $\rho(T)$ was measured by a four-probe method in the temperature interval $4.2 \leqslant T \leqslant 1050$ K. The magnetic susceptibility $\chi_{ac}(T)$ was measured by an induction method at frequencies ranging from 4 Hz up to 2.5 kHz at $T = 4.2 - 300$ K. The amplitude of the ac ®eld ranged from fractions of an oersted to several kOe. The measurements of the magnetization $M(H)$ were performed on a vibrating-coil magnetometer in ®elds up to 14 kOe at temperatures $T = 4.2 \pm 300$ K.

The dynamic properties were investigated by submillimeter quasioptic backward-wave-tube (BWT) spectroscopy[8] in the frequency range $\nu = 5 \pm 20$ cm^{-1} at $T = 5 \pm 300$ K. The transmission $T(\nu)$ and phase $\varphi(\nu)$ spectra of plane-parallel samples with transverse dimensions of 8 ± 10 mm and thickness 0.1 ± 1 mm were measured, and the results were used to determine the complex permittivity spectrum $\epsilon = \epsilon' + i\epsilon''$ or the dynamic conductivity spectrum $\sigma = \sigma' + i\sigma''$ using the well-known formulas for the transmission of a plane-parallel slab.

The results of the measurements of the temperature dependences of the magnetic susceptibility and resistance for different concentrations are presented in Figs. 1 and 2, while Fig. 3 illustrates the temperature behavior of the submillimeter permittivity and dynamic conductivity for $x = 0.125$ together with the static conductivity, magnetic susceptibility, and magnetization. One can see that the temperature dependences of these quantities exhibit a number of anomalies, which are designated in the ®gures by different symbols and which we identi®ed with different magnetic and structural phase transitions. The temperatures of the corresponding phase transformations depend strongly on the composition and are represented in the form of the $T \pm x$ phase diagram in Fig. 4.

The sharp peak in the susceptibility $\chi_{ac}(T)$ (Fig. 1), observed for pure $LaMnO_3$, is due to the antiferromagnetic ordering of Mn^{3+} ions at the Néel point $T_N = 140$ K. Below T_N spontaneous and remanent magnetization appear, attesting to the fact that the magnetic structure is not purely antiferromagnetic but rather weakly ferromagnetic. A similar behavior of $\chi_{ac}(T)$ and the magnetization also occurs for lightly doped compositions ($x = 0.05$ and 0.075), the only difference being that the spontaneous magnetization in this case increases considerably: from ≈ 4 G·cm^3/g for $x = 0$ up to ≈ 17 and ≈ 25 G·cm^3/g, respectively, for $x = 0.05$ and 0.075 at $T = 4.2$ K. This indicates a strong increase in the degree of noncollinearity of the magnetic structure as x increases. The behavior of the antiferromagnetic resonance (AFMR) which we observed in pure and lightly doped

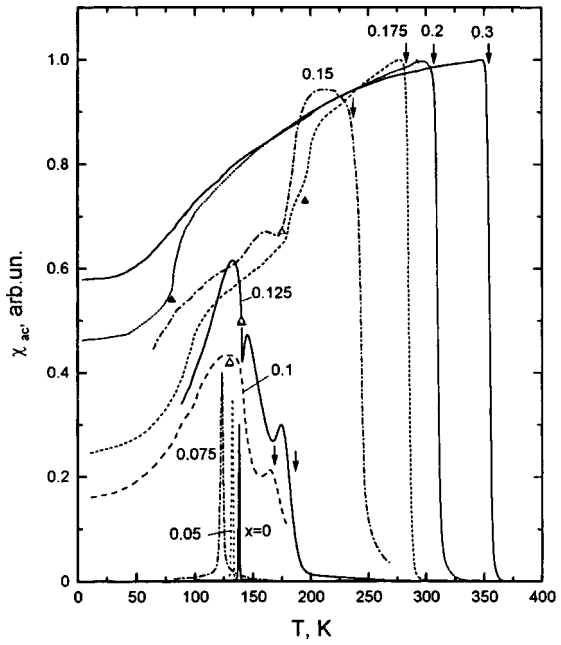

FIG. 1. Temperature dependences of the magnetic susceptibility of $La_{1-x}Sr_xMnO_3$ single crystals. The arrows mark the Curie temperatures; the symbols ▲ mark the temperatures of transitions between the rhombohedral R and orthorhombic O^* phases; the symbols △ mark the temperatures of the transition to the polaron-ordering phase P.

$LaMnO_3$[9] Ð the AFMT frequencies decrease appreciably as the Sr content increases (19 cm^{-1} and 6 cm^{-1} for $x=0$ and 0.05, respectively), while AFMR vanishes for $x \geqslant 0.1$ Ð also indicates suppression of antiferromagnetic order as the doping level increases.

At high doping levels ($x \geqslant 0.15$) the $\chi_{ac}(T)$ curves have a sharp anomaly (marked by the arrow), associated with the appearance of ferromagnetic order at $T=T_C$. As x decreases and T_C decreases (Fig. 4), the ordered state apparently becomes magnetically nonuniform, as is indicated by the smeared character of the transition on the $\chi_{ac}(T)$ curves as $T \rightarrow T_C$ for $x=0.1$ and 0.125. In addition, the maximum susceptibility χ_{ac} is less than the value $1/N$ corresponding to the maximum susceptibility at the Curie point of a homogeneous ferromagnet with demagnetizing factor N. We arrive at the same conclusion also from an analysis of the ®eld dependences of the magnetization: The initial slope of the curves $M(H)$ at temperatures $T<T_C$ is less than that for compositions with $x \geqslant 0.175$, and saturation is not reached in ®elds up to 13 kOe. The nonuniformity of the magnetic state is apparently greatest in the hatched region of concentrations 0.8±0.9 in the phase diagram, where the lines $T_C(x)$ and $T_N(x)$ come together, and here the details of the diagram require additional investigation.

As one can see from Fig. 2, as the Sr content increases, the resistivity at low temperatures decreases from values $\geqslant 10^6\ \Omega \cdot cm$ (the instrumental measurement limit) to $\approx 4.7 \pm 10^{-5}\ \Omega \cdot cm$ for the compound with $x=0.3$. The form of the $\rho(T)$ curves on the whole corresponds to the results of Ref. 2, which were also obtained for single crystals

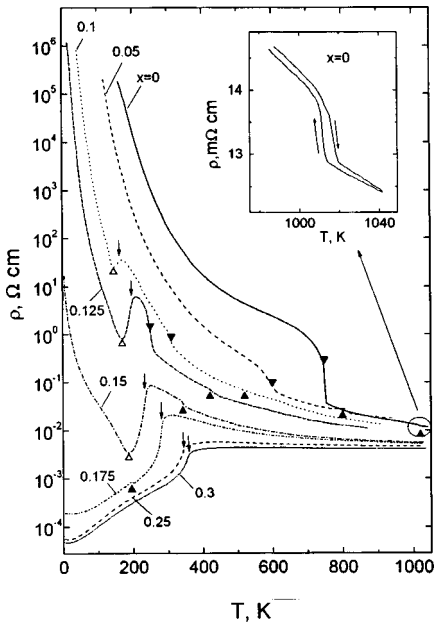

FIG. 2. Temperature dependences of the resistivity ρ of $La_{1-x}Sr_xMnO_3$ single crystals. The arrows mark the Curie temperatures; the symbols ▲ mark the temperatures of the transition between the R and O^* phases; ▼ mark the temperatures of the transition between the two orthorhombic phases O' and O^*; and, △ mark the temperatures of the transition to the polaron-ordering phase P. Inset: Behavior of $\rho(T)$ accompanying a structural phase transition $O^* \rightarrow R$ in pure $LaMnO_3$.

but at temperatures $T < 500$ K. For compounds with $x \geq 0.15$ the value of T_C determined from the anomalies on the $\chi_{ac}(T)$ curves, and the maxima of the magnetoresistance approximately corresponds to the maximum of the derivative $d\rho/dT$. The resistivity minimum, marked by the open triangles, below T_C and the change in the behavior of $\rho(T)$ from metallic to semiconductor behavior, which are observed for compositions with $0.1 \leqslant x \leqslant 0.15$, attest to strong charge-carrier localization at low temperatures and, as neutron-diffraction investigations show,[4] a transition to a polaron-ordering phase P at $T = T_p$. We note that additional anomalies, marked by open triangles, are also observed at this transition on the $\chi_{ac}(T)$ curves for $x = 0.1$, 0.125, and 0.15 (Fig. 1).

Here what is meant by a polaron is a hole in the e_g orbitals of the Mn^{3+} ion (i.e., actually a Mn^{4+} ion), surrounded by a corresponding local distortion of the lattice. Since the Mn^{4+} ion, in contrast to the Jahn±Teller Mn^{3+} ion, does not give rise to strong local distortion of oxygen octahedra, the lattice symmetry increases near such a polaron. According to Ref. 4, the polaron phase P is an ordered arrangement of Mn^{3+} and Mn^{4+} ions for which one of the two alternating atomic layers in the (001) plane contains only Mn^{3+} ions, as in pure $LaMnO_3$, while the other layer contains both Mn^{3+} and Mn^{4+} ions, i.e., holes. For the optimal concentration $x = 0.125$, the holes in this layer occupy 1/4 of the positions of manganese and form a quadrupled (2×2) square lattice with the respect to the initial perovskite cubic cell. As a result, a superstructure with wave vector (1/2, 1/2, 1/4) is formed. This structure apparently remains even in the presence of a small devia-

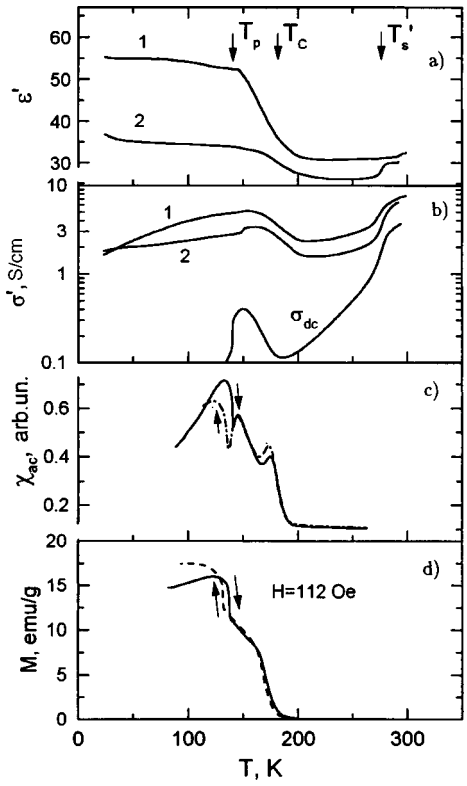

FIG. 3. Temperature dependences of the permittivity $\epsilon'(13.3\ \mathrm{cm}^{-1})$ (a), dynamic conductivity $\sigma'(13.3\ \mathrm{cm}^{-1})$ and static conductivity σ_{dc} (b), magnetic susceptibility χ_{ac} (c) and magnetization M (d) of $La_{1-x}Sr_xMnO_3$. The labels 1 and 2 for ϵ' and σ' correspond to different polarizations of the radiation. The vertical arrows mark the temperatures of the polaron (T_p) and magnetic (T_C) orderings and the structural transition $O' \rightarrow O^*$ (T_s').

tion of the Sr concentration from the optimal value 0.125 (within the range from 0.1 to 0.15).

Besides the anomalies associated with polaron ordering, other anomalies are also observed in the temperature dependences $\rho(T)$ in samples with $x \leqslant 0.2$. We attribute the most pronounced ones, which are marked by the symbols ▼, to a phase transition from a strongly distorted Jahn±Teller orthorhombic phase O' with *Pnma* symmetry ($b/\sqrt{2} < c < a$) to a weakly distorted orthorhombic (pseudocubic) structure O^* ($b/\sqrt{2} \sim a \sim c$) at T_s', relying in so doing on the neutron diffraction data given in Ref. 5 for the composition $x = 0.125$, where the same transition is observed at $T_s' \approx 250$ K. The temperature of this transition increases rapidly as the concentration x decreases and reaches 750 K at $x = 0$, while in the process the resistance changes abruptly by almost an order of magnitude. A similar behavior of ρ at a Jahn±Teller transition in pure $LaMnO_3$ was also observed in Ref. 10.

In addition, we observed in the temperature dependences $\rho(T)$ at higher temperatures a second transition accompanied by a weaker jump in the resistivity and marked by the symbol ▲ in Fig. 2 (see inset for $x = 0$). As x increases, the temperature T_s of this

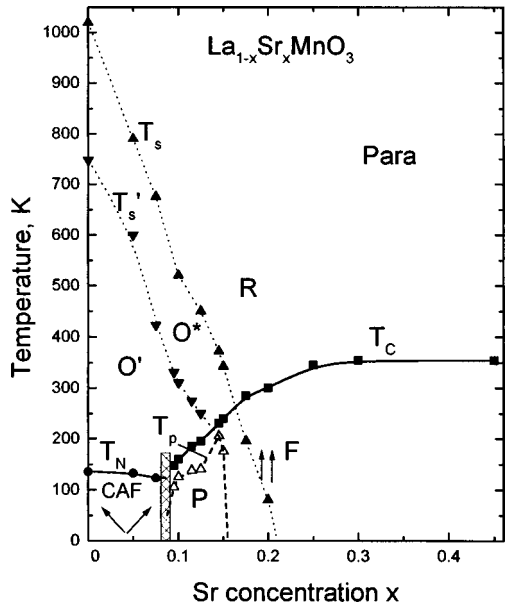

FIG. 4. Structural and magnetic T±x phase diagram of $La_{1-x}Sr_xMnO_3$. R Ð rhombohedral phase; O^* Ð weakly distorted orthorhombic phase; O' Ð strongly distorted (Jahn±Teller) orthorhombic phase; P Ð polaron-ordering phase; Para Ð paramagnetic state; F Ð ferromagnetic state; CAF Ð noncollinear phase; T_C and T_N Ð Curie and NeÂel temperatures; T_s and T_s' Ð temperatures of the transitions $O^* \rightarrow R$ and $O' \rightarrow O^*$, respectively; and, T_p Ð temperature of the transition to the polaron-ordering phase.

transition decreases appreciably, and for $x \geqslant 0.14$ the transition temperatures agree well with published data for a structural transition between orthorhombic O^* and rhombohedral R phases.[2,6] This gives us a basis for identifying the observed transitions as $O^* \rightarrow R$ right down to $x = 0$. In the region of magnetic ordering, for $x = 0.175$ and 0.2, these transitions also manifest themselves in the form of a sharp change in the susceptibility (Fig. 1) and magnetization. Therefore two high-temperature structural phase transitions $O' \rightarrow O^*$ and $O^* \rightarrow R$, corresponding to the lines $T_s'(x)$ and $T_s(x)$ on the phase diagram in Fig. 4, occur in $La_{1-x}Sr_xMnO_3$. The structures of the rhombohedral R and orthorhombic O^* phases are determined by distortions of the initial perovskite cubic structure which are associated with a rotation of the oxygen octahedra around axes of the type [111] and [110], respectively, while the structure of the orthorhombic phase O' is associated with the additional distortion of the O^* phase in the presence of static cooperative Jahn±Teller ordering of the deformed oxygen octahedra.

Let us now turn to the results of submillimeter measurements of the permittivity $\epsilon'(T)$ and dynamic conductivity $\sigma'(T)$, whose temperature dependences for $x = 0.125$ are presented in Fig. 3 for the frequency $\nu = 13.3$ cm^{-1}. The curves 1 and 2 refer to different polarizations of the radiation, which correspond to minimum and maximum transmission. This is evidently associated with the anisotropy of the crystal. It is evident see that appreciable anomalies are observed in the curves $\sigma'(T)$ and $\epsilon'(T)$. They correspond well with the features appearing in the curves of the static conductivity $\sigma_{dc}(T)$, magnetic susceptibility $\chi_{ac}(T)$, and magnetization $M(H)$ (Fig. 3c and 3d) as a result of

phase transitions at T_s', T_C, and T_p. The appreciable increase in $\epsilon'(T)$ after ferromagnetic ordering and a transition to the polaron phase P ($T<T_p$) attests to a substantial transformation of the crystal lattice and apparently a restructuring of the electronic spectrum of the crystal. The latter was observed recently in the optical conductivity spectra σ' for a roughly similar composition ($x=0.1$) and was manifested as the appearance of a maximum of σ' at the frequency ~ 0.5 eV (4000 cm^{-1}) for $T<T_C$,[11] attributed to electronic transitions between the states of the spin-polarized e_g band of Mn^{3+} split by the Jahn±Teller interaction. The strong growth of $\epsilon'(T)$ which we observed at temperatures $T<T_C$ is apparently due to the presence of strong Jahn±Teller spin±lattice coupling and a transition to a polaron-ordered state. We also observed a similar behavior of $\epsilon'(T)$ for compositions $x=0.1$ and 0.15, where ϵ' increased at a transition to the polaron-ordered phase P by the amounts $\Delta\epsilon' \approx 10$ and 50, respectively. At the same time, for the lightly doped compositions $x=0$, 0.05, and 0.075 $\epsilon'(T)$ did not exhibit any anomalies and decreased continuously by 5±15% as the temperature decreased. Therefore the growth (jump) in ϵ' is a characteristic feature of the transition to the polaron phase P, and its boundary with the Jahn±Teller phase O' falls in the concentration range between 0.075 and 0.1.

In summary, it has been shown in this work that the magnetic, dielectric, and conducting properties of $La_{1-x}Sr_xMnO_3$ are closely related, the relationship being most clearly manifested at phase transformations, and the complete T±x phase diagram of this system was constructed.

This work was supported by the Russian Fund for Fundamental Research (96-02-18091, 97-02-17325, and 96-15-96577).

[a)]e-mail: mukhin@ran.gpi.ru

[1] R. von Helmholt, J. Wecker, B. Holzapfel *et al.*, Phys. Rev. Lett. **71**, 2331 (1993).
[2] A. Urushibura, Y. Moritomo, T. Arima *et al.*, Phys. Rev. B **51**, 14103 (1995).
[3] E. L. Nagaev, Usp. Fiz. Nauk **166**, 833 (1996).
[4] Y. Yamada, O. Hino, S. Nohdo *et al.*, Phys. Rev. Lett. **77**, 904 (1996).
[5] H. Kawano, R. Kajimoto, M. Kubota, and H. Yoshizawa, Phys. Rev. B **53**, R14709 (1996).
[6] Y. Moritomo, A. Asamitsu, and Y. Tokura, Phys. Rev. B **56**, 12190 (1997).
[7] J.-S. Zhou, J. B. Goodenough, A. Asamitsu, and Y. Tokura, Phys. Rev. Lett. **79**, 3234 (1997).
[8] G. V. Kozlov (Ed.), *Submillimeter Dielectric Spectroscopy of Solids* [in Russian] (Trudy IOFAN, Vol. 25), Nauka, Moscow, 1990.
[9] V. Yu. Ivanov, V. D. Travkin, A. A. Mukhin *et al.*, J. Appl. Phys. **83**, 7180 (1998).
[10] A. Wold and R. J. Arnott, J. Phys. Chem. Solids **9**, 176 (1959).
[11] Y. Okimoto, T. Katsufuji, T. Ishikawa *et al.*, Phys. Rev. B **55**, 4206 (1997).

Translated by M. E. Alferieff